Catalysis Today 151 (2010) 71–76

Contents lists available at ScienceDirect

Catalysis Today

journal homepage: www.elsevier.com/locate/cattod

Modelling and experimental study of the NO_x photocatalytic degradation employing concrete pavement with titanium dioxide

M.M. Ballari[a,*], M. Hunger[b,1], G. Hüsken[a], H.J.H. Brouwers[a]

[a] Unit of Building Physics and Systems, Department of Architecture, Building and Planning, Eindhoven University of Technology, P.O. Box 513, 5600 MB Eindhoven, The Netherlands
[b] GCC Technology and Processes SA, Ave. des Sciences 1 A, CH-1400 Yverdon-les-Bains, Switzerland

ARTICLE INFO

Article history:
Available online 27 April 2010

Keywords:
Heterogeneous photocatalysis
Nitrogen oxides
Air purification
Concrete roads
NO and NO_2 kinetic model
External influences

ABSTRACT

The photocatalytic degradation of nitrogen oxides (NO_x) employing concrete paving stones with titanium dioxide is studied experimentally and theoretically. Experiments were carried out in a laboratory photoreactor designed according to the standard ISO 22197-1 (2007) [7] to assess photocatalytic materials. A kinetic model is proposed to describe the photocatalytic reaction of NO and NO_2 as well as the influence of several parameters that can affect the performance of the stones, such as NO inlet concentration, reactor height, flow rate, relative humidity and irradiance. The proposed kinetic model is in good agreement with the experimental results, for instance the prediction of the NO and NO_2 concentration at the reactor outlet.

1. Introduction

Photocatalytic reactions constitute one of the Advanced Oxidation Technologies (AOT) applied to water and air purification. This process involves a solid semiconductor catalyst, typically titanium dioxide (TiO_2), which is activated with ultraviolet light (UV) of certain wavelength. TiO_2 in the form of anatase has been the preferred choice due to its strong oxidizing power under UV irradiation, its chemical stability and the absence of toxicity. These reactions are very attractive for treating pollution problems because: (1) in most of the cases they transform pollutants into innocuous products and (2) they have very low selectivity, thus wide range of contaminants can be treated.

Nitrogen oxides (NO_x) is the generic term for a group of highly reactive gases, most of them emitted in air in the form of nitric oxide (NO) and nitrogen dioxide (NO_2). Nitrogen oxides are formed when fuel is burned at high temperatures, as is the case in combustion processes in automobiles. NO_x causes a wide variety of health and environmental impacts, like the formation of tropospheric ozone and urban smog through photochemical reactions with hydrocarbons. Furthermore, NO_x together with SO_x (sulfur dioxide and sulfur trioxide) is the major contributor to the "acid rain", one of the most serious environmental problems across the world.

The European Union (EU) has taken important steps over the past decade leading to a decrease in the emissions to air and water of a number of pollutants. One of its directives (1999/30/EC) [1] establishes limit values for concentrations of sulfur dioxide, nitrogen dioxide and oxides of nitrogen, particulate matter and lead in ambient air. Some of the pollutant emissions have since become more or less manageable; however particulates, NO_x and smog are still problematic.

To date, a number of researchers have investigated the dynamics of the photocatalysis of nitrogen oxides. While some of the NO_x control methodology is to reduce NO_x back to N_2 [2], another approach is to oxidize NO to NO_2, and then NO_2 to HNO_3 through the hydroxyl radical attack generated during the photocatalyst activation stage [3–5]. The development of innovative materials that can be easily applied on structures, with both de-soiling and de-polluting properties, is a significant step towards improvements of air quality. The use of TiO_2 photocatalyst in combination with cementitious and other construction materials has shown a favorable effect in the removal of nitrogen oxides [6].

In the present work, the degradation of NO_x compounds employing concrete paving stones with TiO_2 to be applied in road construction is studied experimentally and theoretically. The experiments were carried out in a photoreactor designed according to standard ISO 22197-1 (2007) [7] to assess semiconducting photocatalytic materials employing NO as the pollutant source. Furthermore, a kinetic model is proposed to describe the photocatalytic oxidation of NO_x (NO and NO_2) and external influences over this reaction. A reaction rate expression for the oxidation of NO as well as for the appearance and disappearance of NO_2 is postulated and the kinetic parameters are determined employing the experimental data. In addition, the influence of several parameters that can affect the performance of these stones, such as NO inlet con-

* Corresponding author. Tel.: +31 40 2472195; fax: +31 40 2438595.
E-mail address: m.ballari@tue.nl (M.M. Ballari).
[1] Tel.: +41 24 423 5391; fax: +41 24 423 5388.

0920-5861/$ – see front matter © 2010 Elsevier B.V. All rights reserved.
doi:10.1016/j.cattod.2010.03.042

Nomenclature

a_v	active area per unit reactor volume ($dm^2\ dm^{-3}$)
A	area (dm^2)
B	reactor width (dm)
C	molar concentration ($mol\ dm^{-3}$)
E	radiative flux ($W\ dm^{-2}$)
H	reactor height (dm)
k	reaction rate constant ($mol\ dm^{-2}\ min^{-1}$)
K	adsorption equilibrium constant ($dm^3\ mol^{-1}$)
L	reactor length (dm)
N	number of experiments or total number of discrete points in the numerical solution of the differential equations (dimensionless)
Q	flow rate ($l\ min^{-1}$)
r	superficial reaction rate ($mol\ dm^{-2}\ min^{-1}$)
RH	relative humidity (%)
t	time (min)
v	velocity ($dm\ min^{-1}$)
V	reactor volume (dm^3)
x	Cartesian coordinate (dm)

Greek letters

α	kinetic parameter related to the irradiance effect ($dm^2\ W^{-1}$)

Subscripts

act	active
air	air
in	inlet condition
NO	nitric oxide
NO_2	nitrogen dioxide
out	outlet condition
w	water

centration, reactor configuration, flow rate, relative humidity and irradiance is investigated. Finally, the model predictions with the estimated kinetic constants are compared with the experimental results obtaining a good agreement between them.

2. Experimental setup and measurements

The recommendations of the standard ISO 22197-1 (2007) [7] were largely followed for the practical conduction of the present study. The applied experimental device is composed of a planar reactor cell housing the concrete stone sample, a suitable UV-A light source, a chemiluminescent NO_x analyzer, and an appropriate gas supply (Fig. 1). Table 1 shows the main characteristics, dimensions and operating conditions of the experimental setup that were employed to carry out the photocatalytic NO degradation experiments. In most of the cases, when one experimental parameter was changed, all other experimental conditions remained standard as presented in Table 1, with the exception of: (i) when the reactor height was changed, a NO inlet concentration equal to $1.34\ mol\ dm^{-3}$ was used instead of the standard value of $4.47\ mol\ dm^{-3}$, and (ii) when the flow rate was changed to $5\ l\ min^{-1}$, experiments for every NO inlet concentration were performed. For more details of the experimental setup employed in this study see [8].

For the development of a kinetic model and the related experiments, one commercial paving stone sample was used. Therefore, differences in measurement results due to varying surface roughness or unequal distribution of catalyst can be neglected. The employed sample is a double layer stone with the upper layer being photocatalytically active. This upper layer was prepared mixing dry powders of normal concrete with TiO_2 powder before adding water to the mixture. Further information about the concrete recipe cannot be provided because it is confidential information of the manufacturing company. In preparation of each experiment, the sample surface is washed with water in order to remove fouling, contamination and potential reaction products due to a previous NO_x degradation. For the measurement, the sample with the reactive surface upwards is placed in the reaction chamber. With the help of an elastic sealing compound all gaps and joints around the sample are caulked that way that the fed air can only pass the reactor along the reactive sample surface. In doing so, a metal sheet of the dimension 87 mm × 192 mm was deployed as a template for the sealing. Then, the active sample surface is kept exactly identical for all measurements.

Table 1
Experimental setup main characteristics and operating conditions.

Description	Standard conditions	Varying parameters
Reactor		
Length (L)	2 dm	–
Width (B)	1 dm	–
Height (H)	0.03 dm	0.02–0.04 dm
Volume (V)	0.06 dm^3	0.04–0.08 dm^3
Photocatalytic stone		
Length (L)	2 dm	–
Width (B)	1 dm	–
UV lamps: Philips compact $S \times 3$		
Input power	25 W	–
Emission wavelength	300–400 nm	–
Flow rate (Q)	$3\ l\ min^{-1}$	$3–5\ l\ min^{-1}$
Relative humidity (RH)	50%	10–80%
Irradiance flux (E)	$10\ W\ m^{-2}$	$0.3–13\ W\ m^{-2}$
NO inlet concentration ($C_{NO,in}$)	$4.47 \times 10^{-8}\ mol\ dm^{-3}$	$(0.45–4.47) \times 10^{-8}\ mol\ dm^{-3}$
NO_2 inlet concentration ($C_{NO_2,in}$)	$0\ mol\ dm^{-3}$	–

After assembling the sample the reactor is closed and the gas supply is started. The UV-A source is switched on as well in order to start the radiation stabilization, but the reactor stays covered to prevent first degradation. With the help of the controls the flow rate and the relative humidity are adjusted. The supplied NO concentration is adjusted to the desired inlet concentration, which is checked by the analyzer. When these conditions appear to be stable the data acquisition is started. Then, the bridge to avoid the photoreactor is closed and the gas flows along the surface of the concrete sample. During this time the measured NO outlet concentration of the reactor first decreases and then approaches again the original inlet concentration. This phenomenon describes the saturation of surface with NO as well as the non-contaminated air removal from the reactor. After this period of time, the reactor cover is removed to allow the UV-radiation passing through the glass. The degradation for the uncovered reactor lasts for 30 min, then the reactor is covered again and the data acquisition is continued for further 5 min. Within the last minutes of measurement the NO and NO_x concentrations return ideally to the original scale. An example of a representative experimental result is shown in Fig. 2, where the different steps mentioned above can be observed.

3. Theoretical model

The photocatalytic oxidation mechanism of NO_x mixtures is reported in several publications (e.g. [3–5]). All of them proposed the NO decomposition to NO_2, and then NO_2 to NO_3H through the hydroxyl radical attack generated during the photocatalyst activation stage (see Table 2). The kinetic expression normally proposed for the NO degradation reaction rate is the

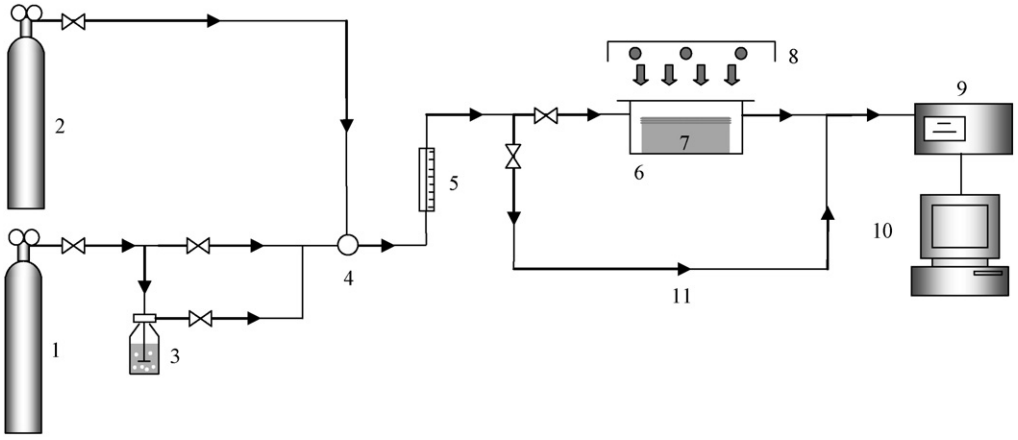

Fig. 1. Schematic representation of the experimental setup. 1. Synthetic air. 2. NO source. 3. Gas washing bottle. 4. Temperature and relative humidity sensor. 5. Flow controller. 6. Gas photoreactor. 7. Paving stone sample. 8. Light source. 9. NO_x analyzer. 10. Computer. 11. Bridge.

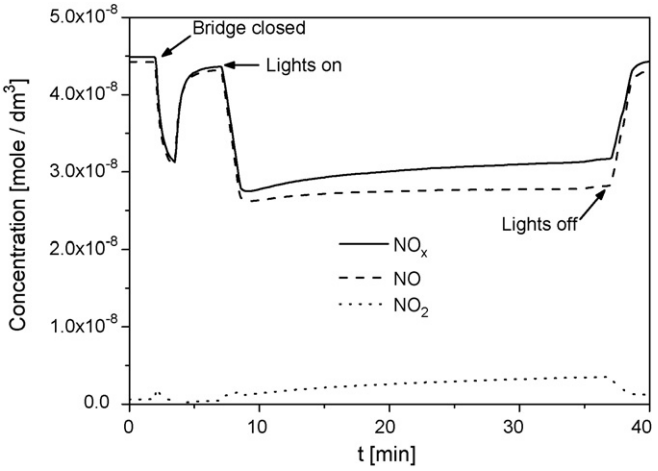

Fig. 2. Representative experimental result. $H = 3$ mm. $Q = 3\,l\,min^{-1}$. $C_{NO,in} = 4.47\,mol\,dm^{-3}$. $E = 10\,W\,m^{-2}$. RH = 50%.

corresponding to the Langmuir–Hinshelwood model [4,5] which is widely employed for the photocatalytic degradation of a large number of contaminants [9,10]. Nevertheless, only a few times the photocatalytic kinetic model includes the reaction dependence with other reactants and/or intermediates concentrations (in this case NO_2) [4]. Moreover, the reaction rate should be expressed as a superficial rate for a gas–solid heterogeneous system [11]. Following this model, applied to a heterogeneous reaction, the Langmuir–Hinshelwood kinetic model for NO disappearance rate and NO_2 appearance/disappearance rate for irreversible reactions, per unit area of active surface and for constant relative humidity and irradiance reads:

$$r_{NO} = -\frac{k_{NO}K_{NO}C_{NO}}{1 + K_{NO}C_{NO} + K_{NO_2}C_{NO_2}} \quad (1)$$

$$r_{NO_2} = -\frac{k_{NO_2}K_{NO_2}C_{NO_2}}{1 + K_{NO}C_{NO} + K_{NO_2}C_{NO_2}} + \frac{k_{NO}K_{NO}C_{NO}}{1 + K_{NO}C_{NO} + K_{NO_2}C_{NO_2}} \quad (2)$$

where r_{NO} and r_{NO_2} are the superficial reaction rate ($mol\,dm^{-2}\,min^{-1}$) of the NO disappearance and NO_2 appearance/disappearance. C_{NO} and C_{NO_2} are the corresponding molar concentration ($mol\,dm^{-3}$) of NO and NO_2 (which are related to the NO and NO_2 concentrations in ppm through the air volume under normal condition of 1 bar and 20 °C). k_{NO} and k_{NO_2} are the corresponding reaction rate constants ($mol\,dm^{-2}\,min^{-1}$) for NO and NO_2. K_{NO} and K_{NO_2} are the adsorption equilibrium constant ($dm^3\,mol^{-1}$) for NO and NO_2, respectively, assuming that these species compete for the same active sites.

Table 2
Photocatalytic reaction mechanism of nitrogen oxides.

Activation	$TiO_2 + h\nu \rightarrow h^+ + e^-$
Absorption	$H_2O_{gas} + Site \Leftrightarrow H_2O_{ads}$ $O_{2gas} + Site \Leftrightarrow O_{2ads}$ $NO_{gas} + Site \Leftrightarrow NO_{ads}$ $NO_{2gas} + Site \Leftrightarrow NO_{2ads}$
Hole trapping	$H_2O_{ads} + h^+ \rightarrow {}^{\bullet}OH + H^+$
Electron trapping	$O_{2ads} + e^- \rightarrow O_2{}^-$
Hydroxyl attack	$NO_{ads} + {}^{\bullet}OH \rightarrow HNO_2$ $HNO_2 + {}^{\bullet}OH \rightarrow NO_{2ads} + H_2O$ $NO_{2ads} + {}^{\bullet}OH \rightarrow HNO_3$
Recombination	$h^+ + e^- \rightarrow$ Heat

Since Hunger and Brouwers [12] have found that this kind of system employing a photocatalytic concrete stone in a flow reactor is not controlled by the interfacial mass transport, a one-dimensional convection-controlled model can be assumed for the NO and NO_2 balance equations:

$$v_{air}\frac{dC_{NO}}{dx} = a_v r_{NO} \quad (3)$$

$$v_{air}\frac{dC_{NO_2}}{dx} = a_v r_{NO_2} \quad (4)$$

where a_v is the active surface area per unit reactor volume:

$$a_v = \frac{A_{act}}{V_{reactor}} \cong \frac{1}{H}[=]\frac{dm^2_{act}}{dm^3_{reactor}} \quad (5)$$

and with the following inlet conditions:

$$C_{NO}(x = 0) = C_{NO,in} \quad (6)$$

$$C_{NO_2}(x = 0) = C_{NO_2,in} \quad (7)$$

3.1. Kinetic parameters estimation

In order to solve the coupled NO and NO_2 mass balances with the kinetic expressions corresponding to Eqs. (1) and (2), a forward discretization of the differential equations (Eqs. (3) and (4)) can be applied (Euler method):

$$v_{air}\frac{C_{NO,i+1} - C_{NO,i}}{x_{i+1} - x_i} = -a_v\frac{k_{NO}K_{NO}C_{NO,i}}{1 + K_{NO}C_{NO,i} + K_{NO_2}C_{NO_2,i}} \quad (8)$$

Table 3
Non-linear parameters optimization employing the Excel Solver tool and the numerical solution of the NO and NO_2 differential mass balance for constant relative humidity and irradiance.

Parameter	Value	95% Confidence interval
k_{NO} (mol dm^{-2} min^{-1})	0.47×10^{-7}	0.01×10^{-7}
K_{NO} (dm^3 mol^{-1})	3.40×10^{7}	0.08×10^{7}
k_{NO_2} (mol dm^{-2} min^{-1})	15.38×10^{-7}	0.02×10^{-7}
K_{NO_2} (dm^3 mol^{-1})	1.24×10^{7}	0.13×10^{7}
N[a]	29	

[a] Number of data.

$$v_{air}\frac{C_{NO_2,i+1}-C_{NO_2,i}}{x_{i+1}-x_i} = a_v\left(-\frac{k_{NO_2}K_{NO_2}C_{NO_2,i}}{1+K_{NO}C_{NO,i}+K_{NO_2}C_{NO_2,i}}+\frac{k_{NO}K_{NO}C_{NO,i}}{1+K_{NO}C_{NO,i}+K_{NO_2}C_{NO_2,i}}\right) \quad (9)$$

So:

$$C_{NO,i+1} = -a_v\left(\frac{k_{NO}K_{NO}C_{NO,i}}{1+K_{NO}C_{NO,i}+K_{NO_2}C_{NO_2,i}}\right)\frac{x_{i+1}-x_i}{v_{air}}+C_{NO,i} \quad (10)$$

$$C_{NO_2,i+1} = a_v\left(-\frac{k_{NO_2}K_{NO_2}C_{NO_2,i}}{1+K_{NO}C_{NO,i}+K_{NO_2}C_{NO_2,i}}+\frac{k_{NO}K_{NO}C_{NO,i}}{1+K_{NO}C_{NO,i}+K_{NO_2}C_{NO_2,i}}\right)\frac{x_{i+1}-x_i}{v_{air}} + C_{NO_2,i} \quad (11)$$

where $i = 1, \ldots, N$ and $L = (x_{i+1} - x_i)(N-1)$.

The optimum values of all kinetic parameters present in Eqs. (10) and (11) for constant relative humidity and irradiance were obtained employing the Excel (Microsoft) "Solver" tool. These results and the 95% confidence intervals are shown in Table 3.

3.2. Relative humidity and irradiance influence

With the objective to incorporate the relative humidity and irradiance effect over the NO_x photocatalytic reaction rate, the previous proposed kinetic model can be extended.

The influence of the relative humidity depends to a large extent on the type of material used. When high values of relative humidity are applied, the hydrophilic effect at the surface is gaining over the oxidizing effect. The water molecules are adsorbed and prevent therefore the adsorption of the pollutants and their reaction with the TiO_2. Therefore, while increasing relative humidity the total efficiency of the system regarding the degradation of NO_x is decreasing [13]. NO_x and water compete for free active sites at the catalyst surface and consequently, water can be considered as an additional reactant and an extended Langmuir–Hinshelwood model can be applied [10]. Therefore, for the present case this extended model could consider the influence of humidity, with the previous K_{NO} and K_{NO_2} as apparent adsorption equilibrium constants in the presence of water vapour:

$$K_{NO} = \frac{K'_{NO}}{1+K_wC_w} \quad (12)$$

$$K_{NO_2} = \frac{K'_{NO_2}}{1+K_wC_w} \quad (13)$$

where C_w is the water molar concentration (mol dm^{-3}) and K'_{NO}, K'_{NO_2} and K_w are the "intrinsic" adsorption equilibrium constants (dm^3 mol^{-1}) for NO, NO_2 and water, respectively.

Regarding the UV-light effect, it is supposed that the irradiance only has an influence on the reaction rate constants for NO and NO_2 (k_{NO} and k_{NO_2}). This assumption is based on the fact that NO and NO_2 degradation takes place through the hydroxyl radical attack. These hydroxyl radicals are formed by the holes trapping with water, after holes are generated during the photocatalyst activation by UV-light (see Table 2). Therefore, a mathematical expression of the reaction constants in function of the radiative flux E can be proposed:

$$k_{NO} = k'_{NO}(-1+\sqrt{1+\alpha E}) \quad (14)$$

$$k_{NO_2} = k'_{NO_2}(-1+\sqrt{1+\alpha E}) \quad (15)$$

with k'_{NO} and k'_{NO_2} (mol dm^{-2} min^{-1}), and α (dm^2 W^{-1}) being factors to be fitted from the experiments. This expression takes account of the linear and the square root dependency of the reaction rate with the light intensity that is announced in several publications [13] for really high and low irradiance, respectively. When UV-radiation is absent, i.e. $E = 0$, the reaction rate becomes zero. For small E, Eqs. (14) and (15) tend to $k'\alpha E/2$, and for large E they tend to $k'\sqrt{\alpha E}$.

Replacing Eqs. (12)–(15) into Eqs. (1) and (2), a complete kinetic model for the photocatalytic degradation of NO_x considering the main factors with influence over the reaction can be obtained:

$$r_{NO} = -\frac{k'_{NO}K'_{NO}C_{NO}}{1+K'_{NO}C_{NO}+K'_{NO_2}C_{NO_2}+K_wC_w}(-1+\sqrt{1+\alpha E}) \quad (16)$$

$$r_{NO_2} = -\frac{-k'_{NO_2}K'_{NO_2}C_{NO_2}+k'_1K'_{NO}C_{NO}}{1+K'_{NO}C_{NO}+K'_{NO_2}C_{NO_2}+K_wC_w}(-1+\sqrt{1+\alpha E}) \quad (17)$$

It is noteworthy that Eqs. (16) and (17) have the same functionality as an extended Langmuir–Hinshelwood model for different reactants competing for the same free active sites [10]. In addition, the derived reaction rates for NO and NO_2 are comparable to the expression obtained by Imoberdorf et al. [13] from a photocatalytic mechanism of an organic pollutant.

Employing the extended reaction rate expressions (Eqs. (16) and (17)), the optimum values of the redefined kinetic parameters were calculated (Table 4). These values are in concordance with those presented in Table 3 and they were obtained employing additional experimental data varying the relative humidity and irradiance.

Table 4
Non-linear parameters optimization employing the Excel Solver tool and the numerical solution of the NO and NO_2 differential mass balance employing the extended kinetic model for relative humidity and irradiance influence.

Parameter	Value
k'_{NO} (mol dm^{-2} min^{-1})	2.96×10^{-6}
K'_{NO} (dm^3 mol^{-1})	8.48×10^{8}
k'_{NO_2} (mol dm^{-2} min^{-1})	1.34×10^{-4}
K'_{NO_2} (dm^3 mol^{-1})	3.02×10^{8}
α (dm^2 W^{-1})	2.37×10^{-1}
K_w (dm^3 mol^{-1})	5.07×10^{4}
N[a]	71

[a] Number of data.

4. Experimental results vs. modelling

It is possible to analyze the effect of different operating variables on the system by resorting the estimated kinetic parameters. This analysis can include a comparison between simulated values obtained with the model and experimental measurements.

Fig. 3 shows the model predictions employing the kinetic parameters presented in Table 3 and the experimental data corresponding to the NO and NO_2 outlet concentration in function of the NO inlet concentration to the reactor for two different flow rates and for constant relative humidity and irradiance (50% and 10 W m^{-2}, respectively). When the inlet concentration of NO

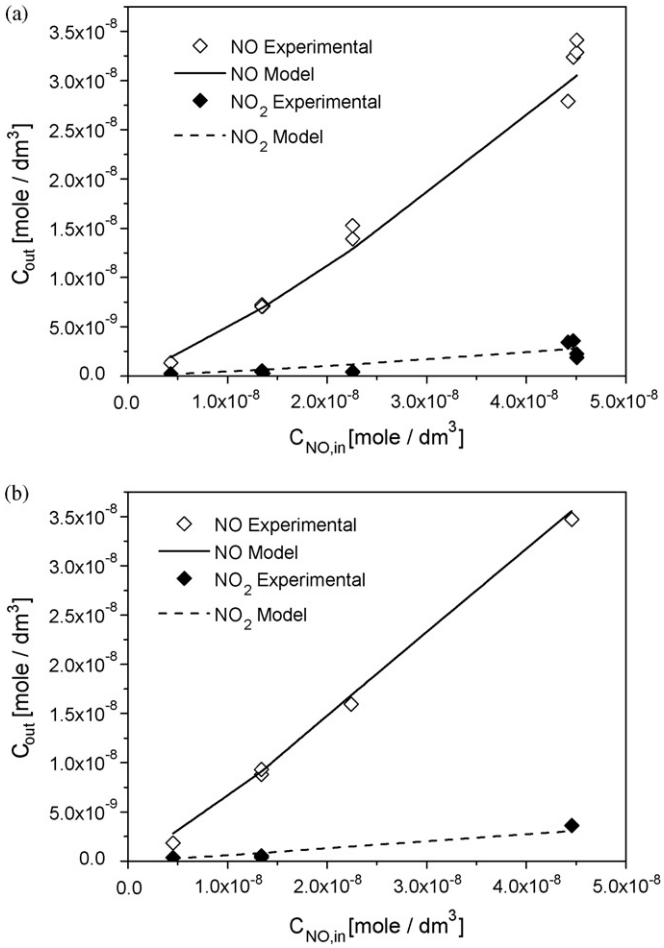

Fig. 3. Model predictions vs. experimental data. NO and NO_2 outlet concentration in function of the NO inlet concentration. $H = 3$ mm. $E = 10\,W\,m^{-2}$. RH = 50%. (a) $Q = 3\,l\,min^{-1}$. (b) $Q = 5\,l\,min^{-1}$.

increases, both NO and NO_2 outlet concentrations rise as well. However, as expected, decreasing the initial concentration of the pollutant the final conversion of the reacting system increases.

The effect of the flow rate is possible to analyze comparing Fig. 3(a) and (b). When the flow rate is increased the resident time in the reactor decreases. Therefore, for low flow rates a larger conversion of the pollutant is observed.

The reactor configuration in the present experimental setup can only be changed varying the reactor height. If the reactor height is varied, no change in the outlet concentration is observed, as NO and NO_2 concentrations are shown in Fig. 4. The explanation of this behavior can be found considering the height effect over the air velocity or resident time and over the total reactor volume. On the one hand, with higher reactor height lower air velocity and longer resident time are obtained resulting in a higher conversion. On the other hand, the reactor volume is larger and for the same photocatalytic active surface a smaller degradation conversion is achieved due to the products dissolution in the gas phase. These parameters (resident time and reactor volume) have opposite effects over the final conversion, resulting in a constant outlet concentration for different reactor heights.

Regarding the irradiance and relative humidity effect, Fig. 5(a) and (b) shows the obtained results varying these two parameters, respectively, and employing the kinetic model presented in Eqs. (16) and (17). When the irradiance is increased a higher conversion of the systems is achieved because more electrons and holes are produced during the photocatalyst activation stage and therefore,

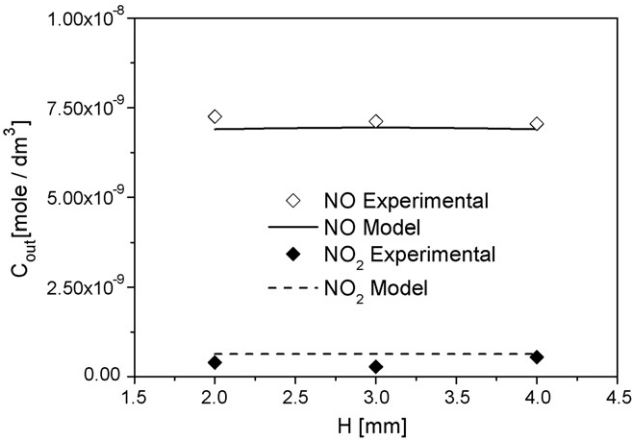

Fig. 4. Model predictions vs. experimental data. Effect of the reactor height over the degradation rate. $Q = 3\,l\,min^{-1}$. $C_{NO,in} = 1.34\,mol\,dm^{-3}$. $E = 10\,W\,m^{-2}$. RH = 50%.

more hydroxyl radicals are formed. However, when the relative humidity is enlarged water competes with NO and NO_2 for the same active sites and the NO_x consumption declines.

Finally, Fig. 6 shows the complete model predictions (Eqs. (16) and (17)) corresponding to the NO and NO_2 outlet concentration in function of the NO and NO_2 experimental data obtained in the photoreactor. These last values should be over a line with a slope

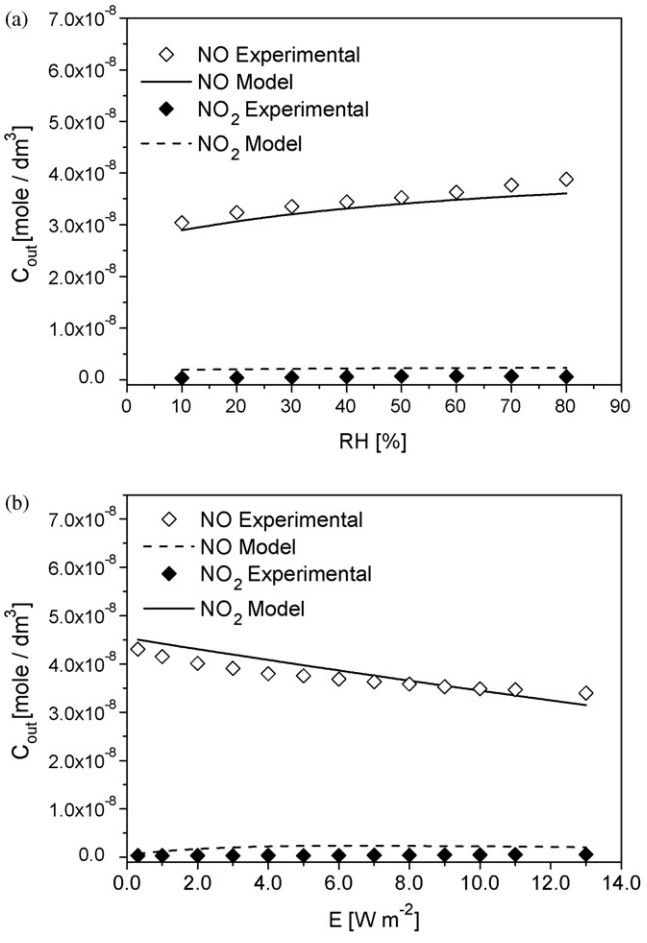

Fig. 5. Model prediction vs. experimental data. $Q = 3\,l\,min^{-1}$. $H = 3$ mm. $C_{NO,in} = 4.47\,mol\,dm^{-3}$. (a) NO and NO_2 outlet concentration in function of the radiative flux. RH = 50%. (b) NO and NO_2 outlet concentration in function of the relative humidity. $E = 10\,W\,m^{-2}$.

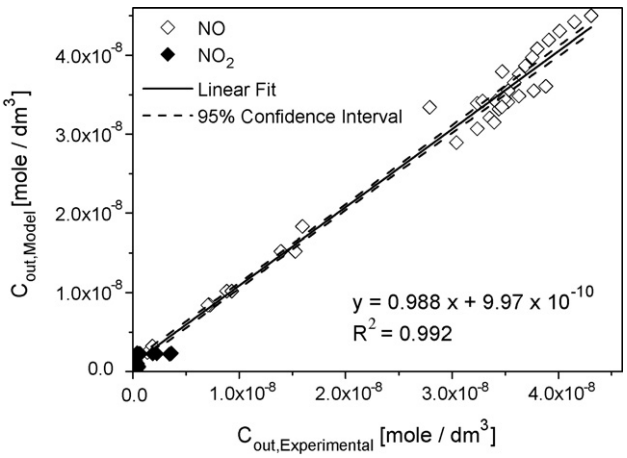

Fig. 6. NO and NO_2 outlet concentration predicted by the complete model including the relative humidity and irradiance effect vs. the experimental data.

close to unity and an ordinate intercept equal to zero, as Fig. 6 shows as well. In all cases, the model predictions show a good agreement with the experimental results.

5. Conclusion

In the present work, a theoretical and an experimental study of the photocatalytic degradation of nitrogen oxides was conducted. A heterogeneous kinetic expression for the NO degradation and for the NO_2 appearance/disappearance was proposed. Several experiments were carried out according to a suitable ISO standard for photocatalytic materials assessment employing only NO as the pollutant. Different operating conditions were selected to carry out the experiments (varying NO inlet concentration, reactor height, flow rate, relative humidity and irradiance). Employing these experimental data and the reaction rate expressions, the kinetic parameters for NO and NO_2 and the main reaction influences were determined. In all cases, a very good correlation between the experimental data and the computer simulations with the estimated kinetic parameters was obtained, allowing to explain the degradation of NO and the apparition of NO_2 in this kind of systems.

Acknowledgements

The authors wish to express their thanks to the following sponsors of the research group: Bouwdienst Rijkswaterstaat, Rokramix, Betoncentrale Twenthe, Graniet-Import Benelux, Kijlstra Betonmortel, Hülskens, Insulinde, Eerland Recycling, ENCI, Provincie Overijssel, Rijkswaterstaat Directie Zeeland, A&G Maasvlakte, BTE, Alvon Bouwsystemen, v. d. Bosch Beton, Twee "R" Recycling and GMB (chronological order of joining).

References

[1] E.U.—The Council of the European Union, Council Directive 1999/30/EC—Relating to Limit Values for Sulphur Dioxide, Nitrogen Dioxide and Oxides of Nitrogen, Particulate Matter and Lead in Ambient Air, 1999.
[2] J. Zhang, Y. Hu, M. Matsuoka, H. Yamashita, M. Minagawa, H. Hidaka, M. Anpo, J. Phys. Chem. B 105 (2001) 8395–8398.
[3] B.N. Shelimov, N.N. Tolkachev, O.P. Tkachenko, G.N. Baeva, K.V. Klementiev, A.Y. Stakheev, V.B. Kazansky, J. Photochem. Photobiol. A: Chem. 195 (2008) 81–88.
[4] S. Devahasdin, C. Fan, J.K. Li, D.H. Chen, J. Photochem. Photobiol. A: Chem. 156 (2003) 161–170.
[5] H. Wang, Z. Wu, W. Zhao, B. Guan, Chemosphere 66 (2007) 185–190.
[6] A. Fujishima, K. Hashimoto, T. Watanabe, TiO_2 Photocatalysis Fundaments and Applications, BKC, Inc., Chiyoda-ku, Tokyo, 1999.
[7] ISO 22197-1, Fine Ceramics (Advanced Ceramics, Advanced Technical Ceramics) – Test Method for Air Purification Performance of Semiconducting Photocatalytic Materials – Part 1: Removal of Nitric Oxide, first ed., 2007.
[8] G. Hüsken, M. Hunger, H.J.H. Brouwers, Build. Environ. 44 (2009) 2463–2474.
[9] D.F. Ollis, in: D.F. Ollis, H. Al-Ekabi (Eds.), Photocatalytic Purification and Treatment of Water and Air, Elsevier Science, Amsterdam, 1993, pp. 481–494.
[10] J. Zhao, X.D. Yang, Build. Environ. 38 (5) (2003) 645–654.
[11] O. Levenspiel, Chemical Reaction Engineering, Wiley, New York, 1999.
[12] M. Hunger, H.J.H. Brouwers, in: M.C. Limbachiya, H.Y. Kew (Eds.), Proceedings International Conference Excellence in Concrete Construction—through Innovation 2008, CRC Press, United Kingdom, 2008, pp. 545–552.
[13] G.E. Imoberdorf, H.A. Irazoqui, A.E. Cassano, O.M. Alfano, Ind. Eng. Chem. Res. 44 (2005) 6075–6085.